UNIVERSITY OF CALIFORNIA,
IRVINE

Particle-Stabilized (Pickering) Emulsions Gels - Structural and Rheological Analysis

THESIS

submitted in partial satisfaction of the requirements
for the degree of

MASTER OF SCIENCE

in Chemical Engineering

by

Zhixuan Xu

Thesis Committee:
Associate Professor Ali Mohraz, Chair
Assistant Professor Mikael Nilsson
Professor Michael Dennin

2014

Dedication

To

the memory of my father

for his endless love and making so many things possible

and

my mother

for her steadfast love and unconditional support

Table of Contents

LIST OF FIGURES

LIST OF TABLES

ACKNOWLEDGEMENTS

I would like to express the deepest appreciation to my committee chair, Professor Ali Mohraz, who guided me to come into the world of colloidal science. I am very much thankful to him for his valuable advice, constructive criticism and his extensive discussion around my work. His encouragement determined me when my steps faltered. Moreover, he always inspires me with new research ideas and teaches me how to think and analyze as an independent researcher. His tremendous assistance in all stages of the writing of my thesis deserves more than words. Without his guidance, encouragement, and patience, this work would not have been possible.

I would like to thank my committee members, Professor Mikael Nilsson and Professor Michael Dennin, for kindly serving in my committee and their understanding, encouragement and personal attention which have provided good and smooth basis for my work.

The support I have received from my colleagues from CSL has also been endearing and I am in awe of their generosity. I gratefully acknowledge the help of Dr. Hubert K. Chan, for providing necessary infrastructure and resources to accomplish my research work. He always provide generously of his advice and experience. I gratefully acknowledge Jessica Witt and Jackie Unangst for implementing the basic concepts which much of my research is based on. I thank them for meticulous training me and allowing me familiar with the environment quickly. I have also enjoyed the numerous discussions on scientific topics with Yi Lu, Max Kaganyuk, Aleksandar Metulev and Leonora Kuzmenko.

Finally, thanks to my parents, my aunt, my uncle and my cousin, Billie Bian, from the bottom of my heart for their endless support and love.

ABSTRACT OF THE THESIS

Particle-Stabilized (Pickering) Emulsions Gels - Structural and Rheological Analysis

By

Zhixuan Xu

Master of Science in Chemical Engineering

University of California, Irvine, 2014

Associate Professor Ali Mohraz, Chair

Emulsions are a group of mixtures made up of two or more immiscible liquids. In 1907, Pickering first described the phenomenon that sufficiently fine-grained solid particles could act as emulsifiers. The solid particles are strongly adsorbed at the liquid-liquid interface to retard droplets coalescence which separates the emulsion into organic and aqueous phase. For a surfactant molecule, the interfacial attachment energy is several k_BT which keeps a dynamic equilibrium between interfaces and host solvent, whereas colloidal particles need to overcome hundreds or thousands of k_BT to detach from the interface. In various fields, such as food, pharmaceutical, cosmetics and personal care products, particle-stabilized emulsions have received significant attention for their potential applications.

After exposing to power ultrasound, particle-stabilized emulsion system could transit into highly stable gel-like emulsions. The gel-like behavior in these systems is a unique result of the

percolating network of droplets that are attached together by a cohesive network of solid particles. The continuous droplet linkage found in particle-stabilized emulsion gels show long-term mechanical stability and resistance to gravitational effects which improve the possibility of improving gel structural life. In addition, the possibility of recoverability for droplet bridging and studies on corresponding microscopic origins and rheological behavior are shown in this work. At macroscopic level, droplet bridging system show stronger structural stability and prolonged mechanical stability.

With a stress-controlled rheometer with cone-and plate geometry, the rheological properties of the emulsion systems were measured. Oscillatory measurement concerning G', the in-phase storage modulus, and G", the out-of-phase loss modulus were taken into consideration in rheological behavior. The higher the frequency is, the lower the modulus crossover strain is; the larger the ratio (aqueous/ organic) is, the higher the strain of crossover modulus is. In the second time strain sweep tests within entire destroyed samples, it shows a unique rheological behavior comparing to original structure. For a group of ratio of aqueous/organic η in colloidal gels, zero shear modulus G'_0 and shear stress τ_y indicate a signature tendency. At small stress range, Pickering emulsion gels exhibit “creep ringing” vibrating behavior; at large enough stress, the strain increases with increasing stress.

Chapter 1

Introduction

1.1 Background

Emulsions are a group of mixtures made up of two or more immiscible liquids. Mostly, emulsions contain both a dispersed and a continuous phase. Common emulsions are kinetically unstable and do not form spontaneously, that is to say, energy input is required to their formation. Overtime, emulsions tend to separate, which is the stable state of the phases comprising the emulsions. Generally, appropriate surfactant molecules are added to reside at emulsion droplet interfaces and result in a decrease of interfacial area. Consequently, the kinetic stability of an emulsion increased. The group of concentrated emulsions shows a striking rigidity, behaving like elastic solids[13].

Pickering first described the phenomenon that sufficiently fine-grained solid particles could act as emulsifiers in 1907[1]. As a result, this type of emulsion was named after S. U. Pickering. In Pickering emulsions, the solid particles are strongly adsorbed at the liquid-liquid interface to retard droplets coalescence which separate the emulsion into organic and aqueous phase[2]. For a surfactant molecule, the interfacial attachment energy is several k_BT which keeps a dynamic equilibrium between interfaces and host solvent, whereas colloidal particles need to

overcome hundreds or thousands of k_BT to detach from the interface[3]. Since the Gibbs free energy to remove solid particle from the interface is much higher than those regular surfactant emulsions, the solid particles are strongly adsorbed at the liquid interface in particle stabilized emulsions[14]. Furthermore, since the interactions between colloidal particles have been well understood, it could be deployed to modify the droplet interactions. Pickering emulsions have received significant attention for their potential applications in food, pharmaceutical, cosmetics and personal care industries.

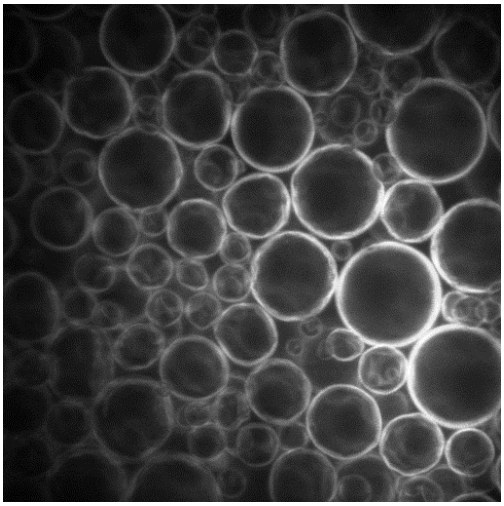

Figure 1.1: Low magnification microscopy images (20×) of Pickering emulsion sample (DI water as aqueous phase).

According to previous work by M. N. Lee et al.[4], highly stable gel-like emulsions could be generated after using an ultrasonic probe operating at 2 W for 20 s continuously. In the first stage of my study, pure DI water served as the aqueous phase. When pure DI water is aqueous phase, the emulsion does not show gel-like behavior after ultrasonication. No bridging formed between droplets with a confocal laser scanning microscope (Figure 1.1). In M. N. Lee et al.[4] work, the aqueous phase was a mixture of dimethylsulfoxide and water (65/35 v/v), and the organic phase was a mixture of toluene and dodecane (18/82 v/v). After being visualized with a

confocal laser scanning microscope, particle bridging across two fluid interfaces and a continuous network of faceted aqueous droplets were observed. The continuous droplet network found in Pickering gels imparts long-term mechanical stability and resistance to gravitational effects which is integral to improve its scaffold life. The gel-like behavior in these systems is a unique result of the percolating network of droplets that are stitched together via a cohesive web of solid particles.

In addition, when a large shear stress was applied to the gel-like self-supporting system, such as vortex mixing, the percolating structure will be destructed. Even with the second ultrasonication, no bridged network could be observed from microscopy, indicating irreversibility of such percolating network.

This interesting phenomenon inspires us to explore the possibility of recoverability for droplet bridging and conduct studies on corresponding microscopic origins and rheological behavior. Thus, an in-depth understanding of bridged Pickering emulsion gels flow properties is of both fundamental interest and of value for various potential applications.

In my project, nearly monodisperse para-Methoxy-N-methylamphetamine (PMMA) particles are utilized to stabilize aqueous phase in organic phase Pickering emulsions, protruding from the interface to create droplet bridging after ultrasonication.

Macroscopically, droplet bridging system can impart prolonged mechanical stability. Thus, we become interested in the rheological behavior of this system, and we do perform rheology testing on it. Complicated mechanics related to deforming, rearranging, and breaking the soft building blocks that are brought together by fine solid particle layer might lead to unique rheology in solid-stabilized emulsions with bridged droplets. As a result, a thorough

experimental assessment of this phenomenon and the system's microstructural origins would be of great interest to the wide host of technologies that utilize Pickering emulsions and can smooth the path for the synthesis and engineering of new multiphase mixtures with enhanced stability, morphology, and rheological properties. Fine spatial resolution is indispensable to acquire emulsion microstructure. However, the inherent abundance of scattering surfaces in this multiphase system brings about challenges of direct visualization and qualification of its morphology. It has limited the establishment of connection between microstructure and rheology. To reach the test requirements of imaging, a model solid-stabilized emulsion that has been carefully designed in the laboratory is needed.

1.2 Structure of the Thesis

In this thesis, a series of structural and rheological analysis was conducted over a Pickering emulsion gel system. From the perspective of structure, droplet radius formula was derived (Chapter 2.2.2). The microscopic origins were observed and interpreted by a confocal laser scanning microscope (Chapter 2.2.3). Rheological behavior analysis was mainly based on oscillatory tests and creep experiments using a stress-controlled rheometer (Chapter 3).

Chapter 2

Structural Analysis of Particle-Stabilized (Pickering) Emulsions Gels

2.1 Introduction

Sitting on a fluid-fluid interface, the equilibrium position of a colloidal particle can be characterized by the three-phase contact angle, θ, which correspond to the governing surface free energies. Typically, interfacial adsorption is irreversible, when colloidal particles possess near-neutral wetting properties (θ≈90°). Partially hydrophobic particles with θ somewhat greater than 90 °tend to stabilize water-in-oil (w/o) emulsions where particles slightly protrude from droplet surfaces to maintain the equilibrium contact angle. In our Pickering emulsion gel system, the stabilizer consisted of graft-copolymer chains of poly-(dimethylsiloxane)-*g*-poly (methyl methacrylate) (PDMS-*g*-PMMA). A confocal fluorescence microscope was used to visualize the microstructure of particle-stabilized emulsion gels.

2.2 Methodology of Structural Analysis

2.2.1 System Composition

Nearly monodisperse PMMA with an average radius of r_d=0.9μm is applied to stabilize w/o Pickering emulsions, protruding from the interface to create droplet bridging. Emulsion systems with specific particle volume fraction φ_p and volume ratio of the aqueous to organic

phase η were prepared by dispersing dry PMMA particles in a two–phase liquid mixture. Vortex mixing and ultrasonication bath were used to mix the system well. Then an ultrasonic probe (Branson Sonifier 250) was operated on the sample at 2W with 80 % duty cycle. We started from a system with pure water as aqueous phase to explore the possible system composition.

To ensure the visualization of the local microstructure at certain depths in samples, the composition of each fluid phase was chosen to match the refractive index of the particles approximately. The systems we plan to work on using a mixture of two different organic phases, dodecane and decalin. The separate refractive indices are shown in Table 2.1.

Components	Refractive Index
Water	1.333
Decalin	1.469~1.481
PMMA Particle	1.49

Table 2.1: Refractive indices of components in system.

To coincide the refractive indices of the liquid phases with solid particles, allowing 3D microstructural characterization of the mixture by confocal microscopy, the aqueous phase ought to be tuned to increase. To bring up the refractive index of the aqueous phase, sodium iodide was dissolved in DI water at a total concentration of 60% by mass. It is based on the correlation between concentrations of sodium iodide solution aqueous solution and refractive indices[5]. Under typical ranges of ambient conditions, T. L. Narrow et al. developed a simple model from experimental measurements. Figure 2.1[5] Relationship between NaI concentration and the index of refraction of NaI solution: real data and predictions are shown at temperature = 20 ℃ for λ = 589.3 and 632.8 nm and at temperature = 25 ℃, 30 ℃ and 35 ℃ for λ=589.3 nm.

Besides, the colloidal surface chemistry also needs to be carefully tuned to allow the stabilization of two interfaces by each particle through bridging. Under such conditions, the mixture can form a network of colloid-stabilized droplets with the majority of particles being

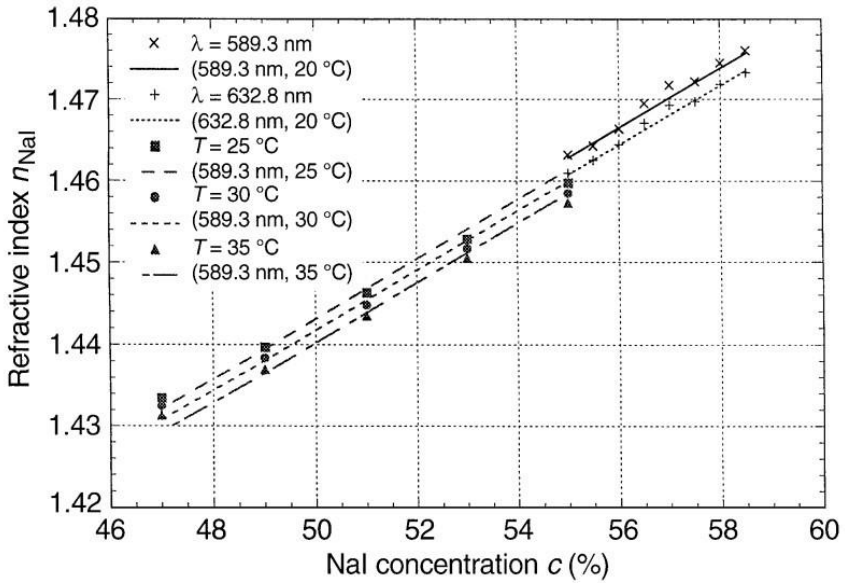

* T. L. Narrow, Experiments in Fluids 28 (2000) 282-283
Figure 2.1: Plot of n_{NaI} vs. c. Experiment data are denoted by different symbols; the model predictions are plotted as various lines

shared by neighboring droplet pairs. Generally, the microstructures of emulsion bear a striking resemblance to a colloidal gel except for the replacement of colloidal building blocks with solid-stabilized droplets. In the light of the microstructural origins of gel-like rheology in this intriguing class of soft materials, the finding from the rheological behaviors might be well interpreted.

Sample before and after ultrasonication is shown in Figure 2.2(a). The composition is shown in Table 2.2. Ultrasonication switched the original color of the sample from pink to orange. It will not affect the image quality of the sample. While vortex mixing only did not generate color change, this transition was achieved only by ultrasonication.

	m_{NaI}	m_{PMMA}	V_{H2O}	$V_{Decalin}$
Fig 2.2 Sample	0.6000g	0.0800g	0.4ml	1.5ml

Table 2.2 Composition of Sample

Since sodium iodide is reductive, it could be easily oxidized and iodine separates out from the aqueous solution. Therefore, a possible explanation was that iodine separate from aqueous phase and some of the salt partition into the oil phase. Combining the pink color of PMMA particles and yellow/brown color of iodine, the bright orange color of the droplets layer was created.

Figure 2.2: (a) Sample after ultrasonication (Left) and before sonication (Right); (b) Status of Sample (0.6g NaI dissolves in aqueous phase) after sonication

The colored part occupied upper layer of the system with simply vortex mixing. With an ultrasonic probe, the droplets part fell to the lower layer.

Upon ultrasonication, the experimental group samples immediately transited from a multiphase liquid-like mixture to a more dense (solid-like) mixture (Figure 2.2 (b)).

2.2.2 Droplet Radius Formula

To derive a formula of droplet radius, a structural model and several assumptions need to be constructed. The schematic representation of droplet structure by PMMA particles is shown in Figure 2.3.

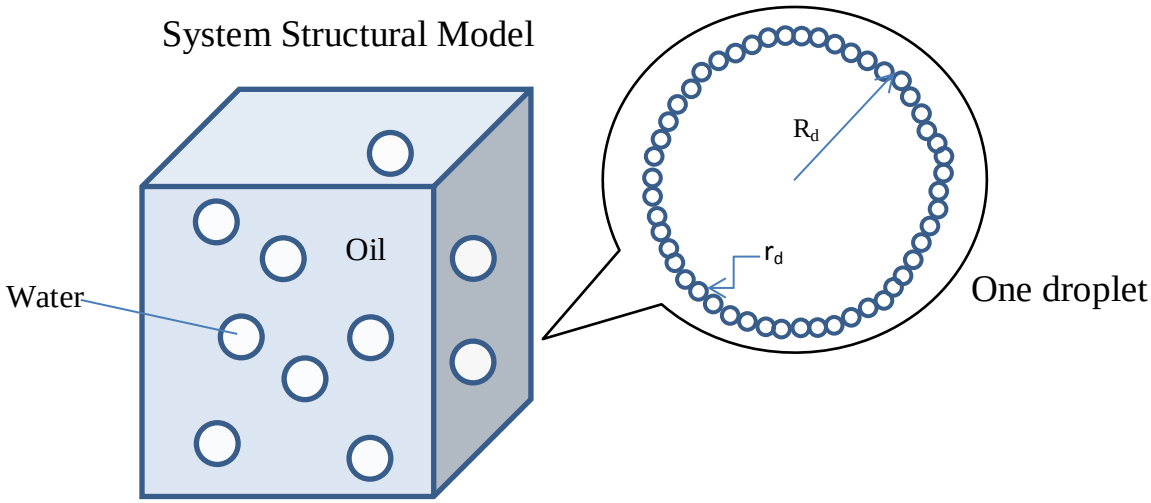

Figure 2.3: The schematic representation of droplet structure

To derive the equation of droplet size before ultrasonication, we assume droplets formed in the system share same droplet size and particles occupied the surface of droplets with a hexagonally close-packed mode. The droplet size equation is as follows:

$$R_d = \frac{\frac{\eta}{\eta+1} V r_d \rho_{PMMA} \frac{\pi}{2\sqrt{3}}}{m_{PMMA}} = \frac{\frac{\eta}{\eta+1} r_d \frac{\pi}{2\sqrt{3}}}{\varphi_p}$$

Total Volume of the System V/ml

Volume Ratio of the Aqueous to Organic Phase η

Radius of Stabilized Particles (PMMA) r_d

Density of Stabilized Particles (PMMA) ρ_{PMMA}

Total Mass of Stabilized Particles (PMMA) m_{PMMA}

Particle Volume Fraction φ_p

Droplet Size R_d

A confocal microscope was applied to get real time image of individual droplets. After using a specific scheme to convert pixel number to real length, an average droplet radius is approximately equal to 40μm.

Fps	m-20x	m-20x (Old)	m-100x	m-100x (Old)
29	0.52670	0.61187	0.10902	0.12949
50	0.45358	0.54560	0.09483	0.11412
65	0.39673	0.48858	0.08336	0.094669
76	0.35088	n/a	n/a	n/a
86	0.32042	0.40588	0.06526	0.078594
93	0.28454	n/a	n/a	n/a
99	0.26675	0.34535	0.05461	0.073948
104	0.24313	0.32118	0.04977	0.069285

Table 2.3 Previous and revised conversions

When we try to correlate the theoretical derivation with linear trend line from confocal microscopy, an inexplicable intercept exists in the trend line (Figure 2.4).

When we try to interpret the deviation, the three possibilities are:

1) Images we got are based on different sample layer. Droplets in sediment layer have larger radius;

2) Inaccurate conversion between pixels in images and real sizes;

3) The assumption, PMMA particles are packed covering the surface of the droplet, cannot describe the system well enough. A portion of particles do not join the droplet formation.

Thus, we calibrated the conversion between pixels and length. The working equations for the 20x and 100x objectives are as follows. These equations are of the form y=m/x and give you

the pixel size in μm (y) as a function of the digital zoom (x). The values of m for different scan rates are as follows:

Applying the revised conversion, we could compare linear relationship change of the equation. The intercept value decrease but could not reach the origin of coordinates (Fig. 2.4).

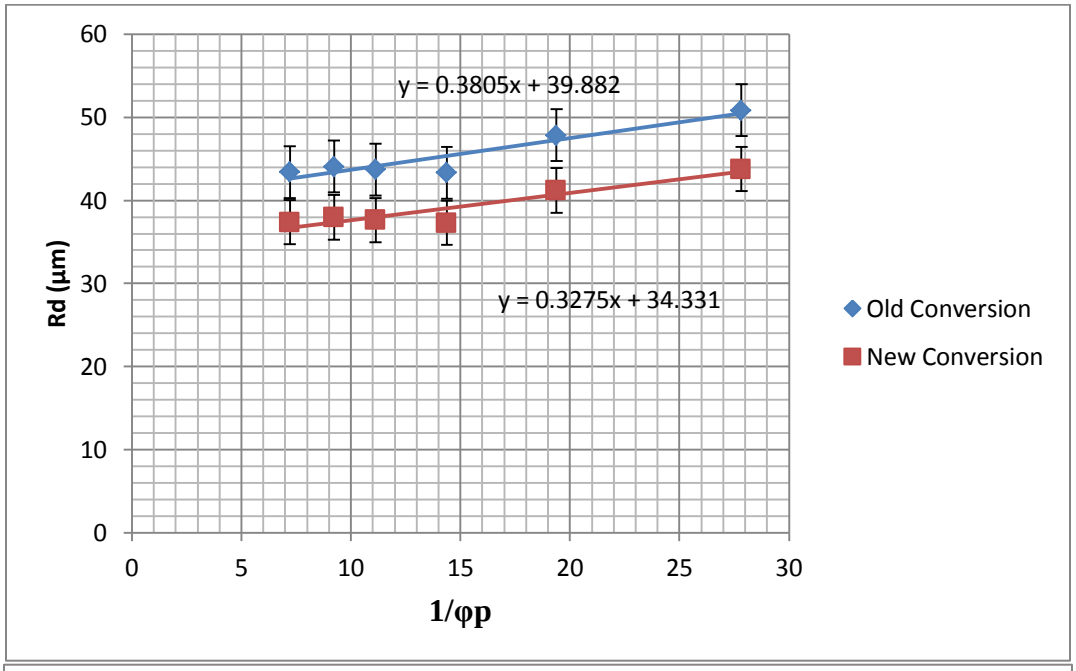

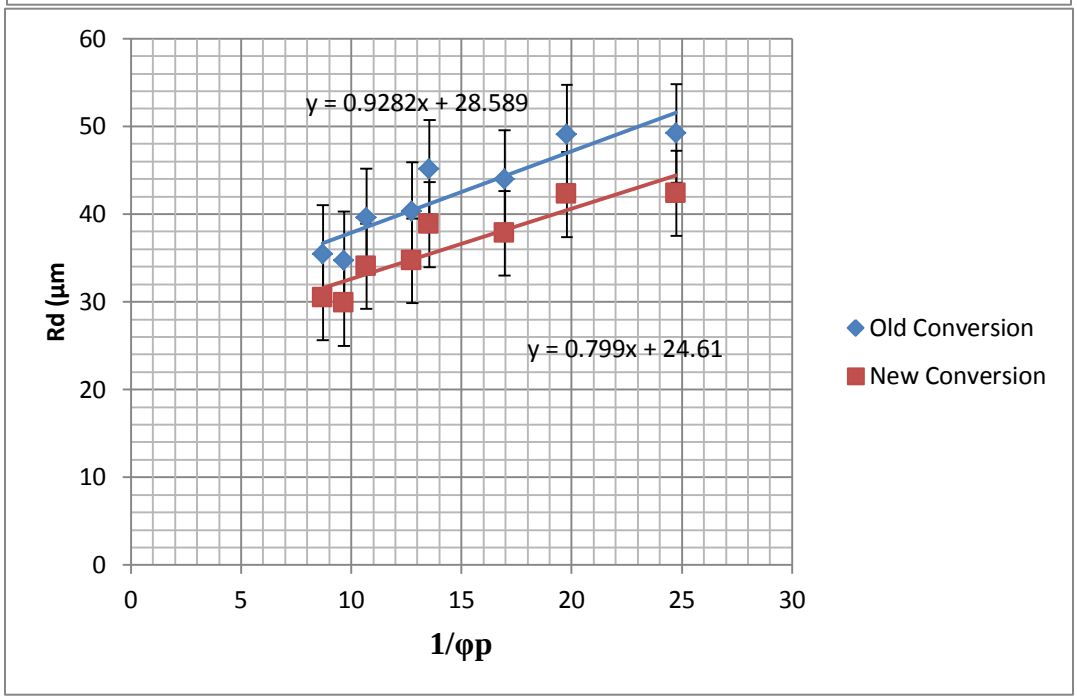

Figure 2.4 Linear relationship between particle volume fraction and droplet radius using previous and revised conversion

Longer vortex mixing time, much more particles join the formation of droplets. Figure 2.5 indicates that even though our systems have been mixed well enough, it is inappropriate to ignore the number of free particles.

In fact, the particle packing shape is irregular result in non-ordered packings[11].

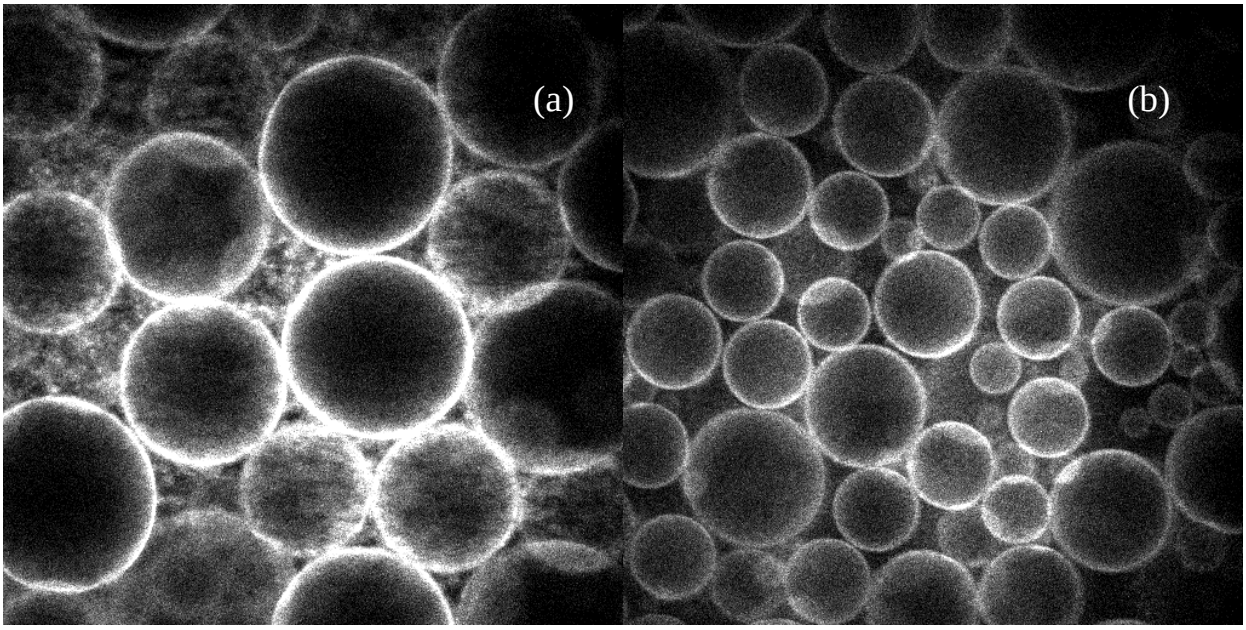

Figure 2.5: Confocal microscopy images (20x) for droplets (5%, 40/60) with different vortex mixing time. a) Short time (7~8min) and b) Longer time (20min).

M. N. Lee et al.[4] went through three strategies for tuning the microstructure of Pickering emulsions gels. They drew conclusions that an increase in the volume ratio of the aqueous (dispersed) to organic (continuous) phase (η) at a constant particle volume fraction (ϕ_P) produces successively larger droplets; an increase in ϕ_P at constant η reduces the droplet size; a proportional increase in both ϕ_P and η increases the volume fraction of droplets without affecting their size. Theoretically, our derivation is consistent with the conclusion they made before.

2.2.3 Microscopic Observation

2.2.3.1 Structural Stability

In order to study the structural stability of particle-stabilized emulsion gel scaffold, experimental design included two different system compositions and at various time points.

Under low magnification, microscopic images were obtained from sample with η = 50/50 and φ_p = 5.898%. Figure 2.6 (a) shows almost perfect sphere shape of droplets after vortex mixing only; when it comes to the moment right after ultrasonication in Figure 2.6 (b), droplets exhibited irregular sphere shape and average droplet size had an obvious decrease than before ultrasonication.

In order to examine short-term structural stability, sample was allowed to stand for four hours before Figure 2.6 (c) was obtained.

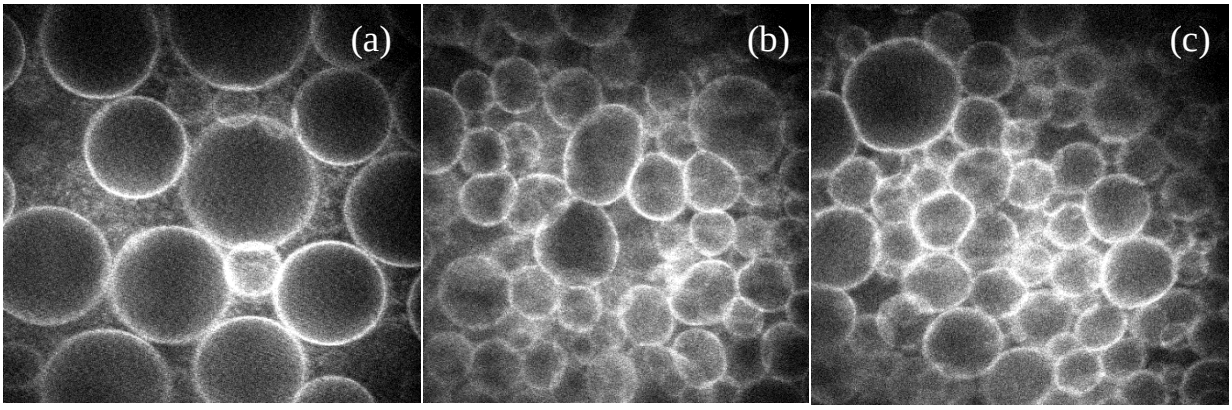

Figure 2.6: (a) 20x images before ultrasonication; (b) right after ultrasonication; (c) 4h after ultrasonication (η = 50/50, φ_p=5.898%)

Droplets exhibited irregular sphere shape, however, average ovality of droplets are smaller than newly made emulsion gels. A possible explanation is structure tend to keep lower energy status. Droplets with higher ovality have higher energy, thus irregular droplets have a

tendency to be sphere with longer time. Average droplet size also had an obvious decrease than non-ultrasonicated samples; simultaneously, it shows similar size with newly made ultrasonicated samples.

Under high magnification (100×), microscopic images were obtained from sample with η = 40/60. In order to examine long-term structural stability, sample was allowed to stand for a week before Figure 2.7 (c) was obtained.

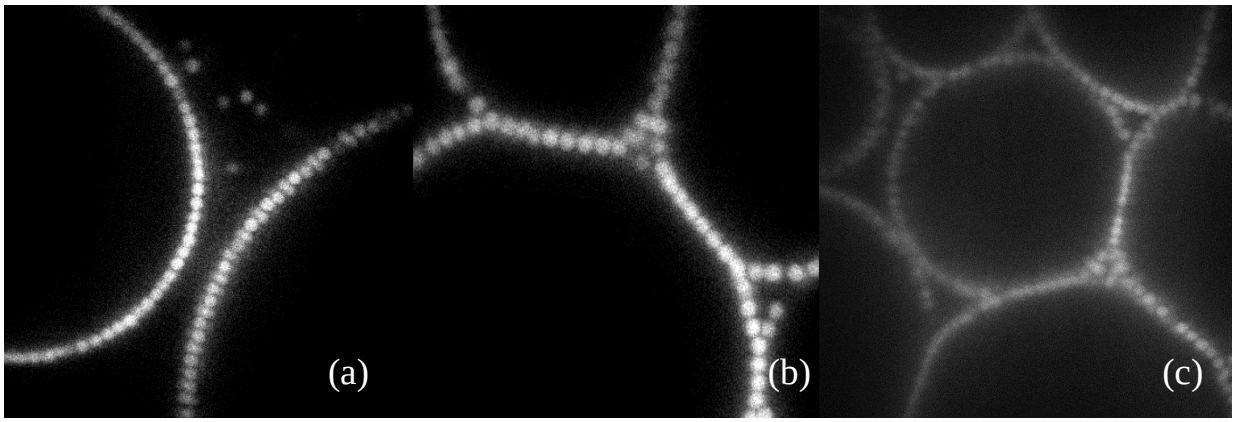

Figure 2.7: (a) (b) 100x images right after ultrasonication; (c) a week after sonication (η = 40/60, m_{PMMA}=0.0804g)

From Figure 2.7, it could be easy to distinguish part of the droplets formed bridging from their neighbors in sample after ultrasonication. When taking long-term structural stability into consideration, no obvious bridging behavior and droplet shape differences could be observed.

In Figure 2.7 (a), the two layers of PMMA on separate droplets indicated no bridging between those two droplets. In Figure 2.7 (b), there were monolayer PMMA particles on right hand side, while there were two layers of PMMA between central droplet and neighbor droplet in the bottom left corner. Whereas, in M. N. Lee *et al.*[4] study, they obtained a stronger bridging between droplets. Polygonal droplets could be distinguished easily from their confocal

microscope pictures. We could draw a conclusion that our systems receive partial weak bridging after being ultrasonicated.

2.2.3.2 Structural Recoverability

In order to study the structural recoverability of particle-stabilized emulsion gel, a second time ultrasonication was applied after vortex mixing samples already had been ultrasonicated. To examine the layer of PMMA particles, high magnification (100×) was applicable.

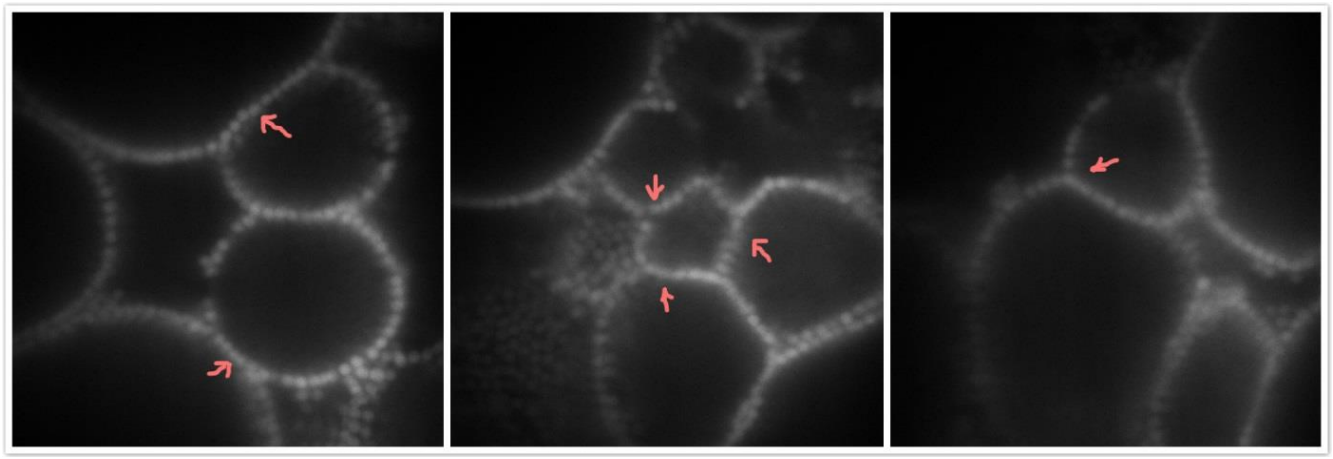

Figure2.8: (100x) Microscopic imaging of different locations after ultrasonicating the 2nd time, vortex mixing after 1st ultrasonication, ensure structure entirely destroyed

Systems with sodium iodide aqueous phase were vortex mixed after the first time ultrasonication. After we ensure that its structure has been entirely destroyed, sample went through ultrasonication again. High magnification microscopy images from different locations are provided in Figure 2.8. Based on Figure 2.8, we could find some droplets shared monolayer PMMA boundaries with their neighbors. If the second-time ultrasonication was applied to destroyed gel-like samples, partial weak bridging was formed again in our system.

2.3 Summary

In this chapter, derivation of droplet radius formula, microscopic observation and interpretation based on structural analysis scope is demonstrated. Droplet radius formula on basis of theoretical system structural model is derived. To correct the deviation between theoretical model and actual size, conversion calibration and inaccuracy in assumption are taken into consideration. Necessary corrections and conditions are made to be supplementary to the formula. Two structural characteristics, stability and recoverability, are considered by microscopic analysis. Both in short-term and long-term, Pickering emulsion gels show relative strong structural stability with low level microstructural change with time. When a second time ultrasonication was applied to destroyed Pickering emulsion gels, partial weak bridging was recovered in the system.

Chapter 3

Rheological Analysis of Particle-Stabilized (Pickering) Emulsions Gels

3.1 Introduction

In rheology, two parameters, G' is the in-phase storage modulus and G" is the out-of-phase similarly-directed loss modulus; The G’ represents the solid properties of the gels while the G” represents the liquid properties. The storage and loss moduli (G’ and G’’, respectively) were recorded throughout both tests. It follows that, $\tan(\delta) = G''/G'$. The value, $\tan(\delta)$, quantifies the balance between energy loss and storage. As $\tan(45°) = 1$, a value for $\tan(\delta)$ greater than unity indicates more "liquid" properties, whereas one lower than unity means more "solid" properties, regardless of the viscosity. The zero-shear elastic modulus, G'_0, was estimated as the average value of G’ over the range of $0.005\% < \gamma < 0.01\%$. The yield stress, τ_y, was defined as the stress value at which G’ = G’’. In the rheology tests, it is shown by the crossover points of oscillatory strain sweep of the systems.

Frequency dependence of the dynamic modulus, $G'(\omega)$, may span over a very wide frequency range, covering many decimal orders of magnitude. In this case, values of G’ also vary in a wide range. For many polymeric substances, there is frequency range where G’=const. which plays an important role in mechanical characterization of materials[6]. For our multiphase systems, the frequency range also characters the mechanical properties of materials.

3.2 Methodology of Rheological Analysis

The rheological properties of the emulsions were measured on a stress-controlled rheometer with plate geometry, and a solvent trap was utilized to minimize evaporation at the set environmental measurement temperature of 25 ℃.

Emulsions with particle volume fraction φp and volume ratio of the aqueous to organic phase η were prepared by dispersing dry PMMA particles in a two – phase liquid mixture. Vortex mixing and sonication bath were used to mix the system well. Then an ultrasonic probe (Branson Sonifier 250) was operated on the sample at 2W for 20s at 80% cycle. Each fluid phase of the system ought to be chosen to match the refractive index of the particles approximately to ensure the visualization of the local microstructure at certain depths in samples. To bring up the refractive index of the aqueous phase, sodium iodide was dissolved in DI water at a total concentration of 60% by mass. The organic phase was Decalin (decahydronaphthalene). The imaging will be performed on a confocal microscope (Axio Observer, Carl Zeiss Microimaging, Inc.) for non-sonicated, newly sonicated and shear systems. The rheological properties of the emulsions were measured on a stess-controlled torsional rheometer (AR-G2, TA Instrument) with plate geometry (d=25mm). The sample was gently poured and spread on the glass plate and the cone was lowered slowly to avoid destruction of the structure. When the system deviates from linearity, at different strains, elastic modulus G’ and viscous modulus G’’ are obtained by the rheometer software TRIOS. Physical interpretation of the modulus numbers will be based on images. The rheo-imaging method is applied to theoretical studies of microscopic and bulk characteristics.

3.2.1 Strain Sweep - Pre-Experimental Design

Pre-experimental design was applied at the first stage of rheometer testing. In order to get more exact test range and meaningful constant values of frequency sweep and strain sweep, several groups of rheometer tests were performed.

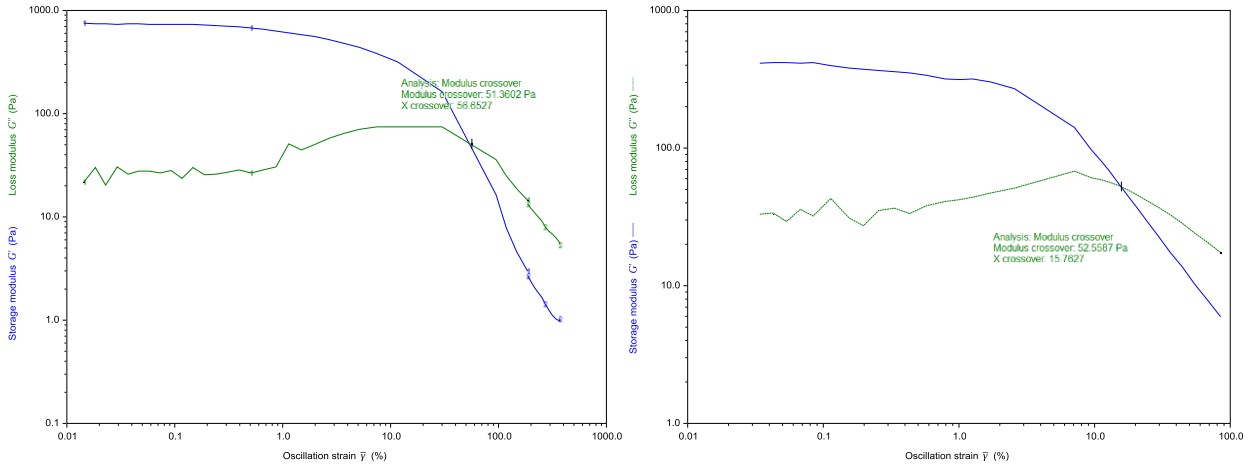

Figure 3.1. Strain – Sweep profiles for the Pickering emulsions (η=40/60, 60% NaI aq phase) at ω =10 rad/s (Left) and 15 rad/s (Right)

Strain-sweep profiles for the Pickering emulsions (η=40/60, 60% NaI aq phase) at angular frequency = 10 rad/s and 15 rad/s were shown in Figure 3.1.

A small peak in G'' is visible around a strain of 10%.

By analyzing storage modulus (G'/Pa, Blue Line) and loss modulus (G''/Pa, Green Line) of samples, the higher the angular frequency value is, the lower the modulus crossover strain is. Simultaneously, effects of strain changes on modulus crossover value seems to be weak (Gcrossover =51.3601Pa, at **ω** =10 rad/s; Gcrossover =52.5587Pa, at **ω** = 15 rad/s).

3.2.2 Oscillation Test – Characteristic Behavior

A group of series η ultrasonicated samples were prepared with η=20/80, 30/70, 40/60 and 50/50. After ultrasonication, each sample first went through a frequency sweep from f=0.1Hz to

80Hz with a constant oscillatory strain of γ=0.1%, followed by an oscillatory sweep γ=0.005 to 100% at a constant f=1Hz. After destroy the structure entirely, repeat the previous two tests to compare rheological characteristics of original bridging and recovered bridging. The storage and loss moduli (G' and G'', respectively) were recorded throughout both tests.

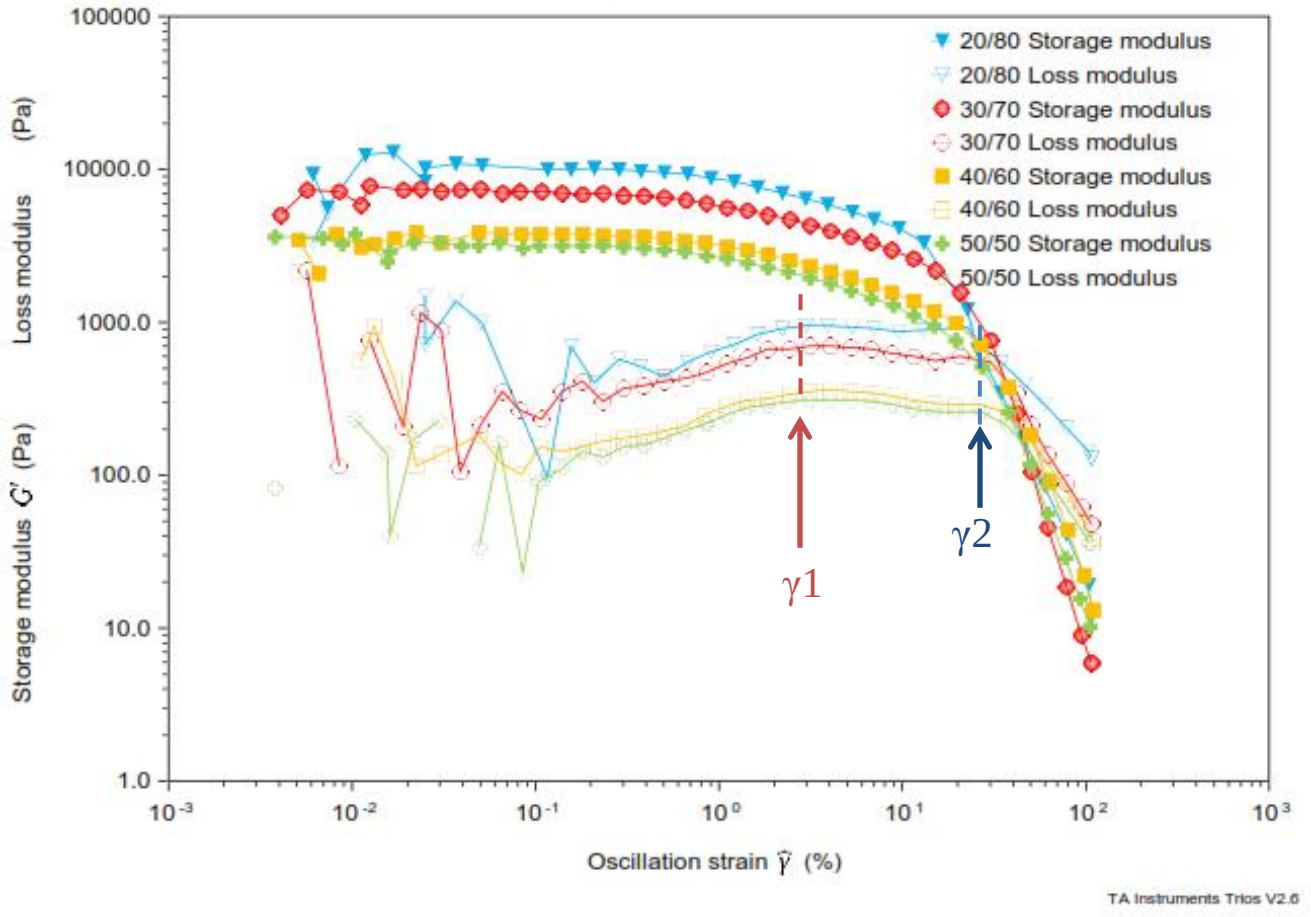

Figure 3.2: Rheology of Pickering emulsion gels. Strain sweep profiles for 5% particle volume fraction systems with 20/80, 30/70, 40/60 and 50/50 ratio. Storage modulus values are denoted by filled symbols; loss modulus values are denoted by open symbols; blue, red, orange and green with respect to 20/80, 30/70, 40/60 and 50/50 ratio.

Two peaks in G'' at γ_1 (dark red arrow) ≈3%, γ_2 (navy arrow) ≈30% could be located in our droplets emulsion gel systems (Figure 3.2)

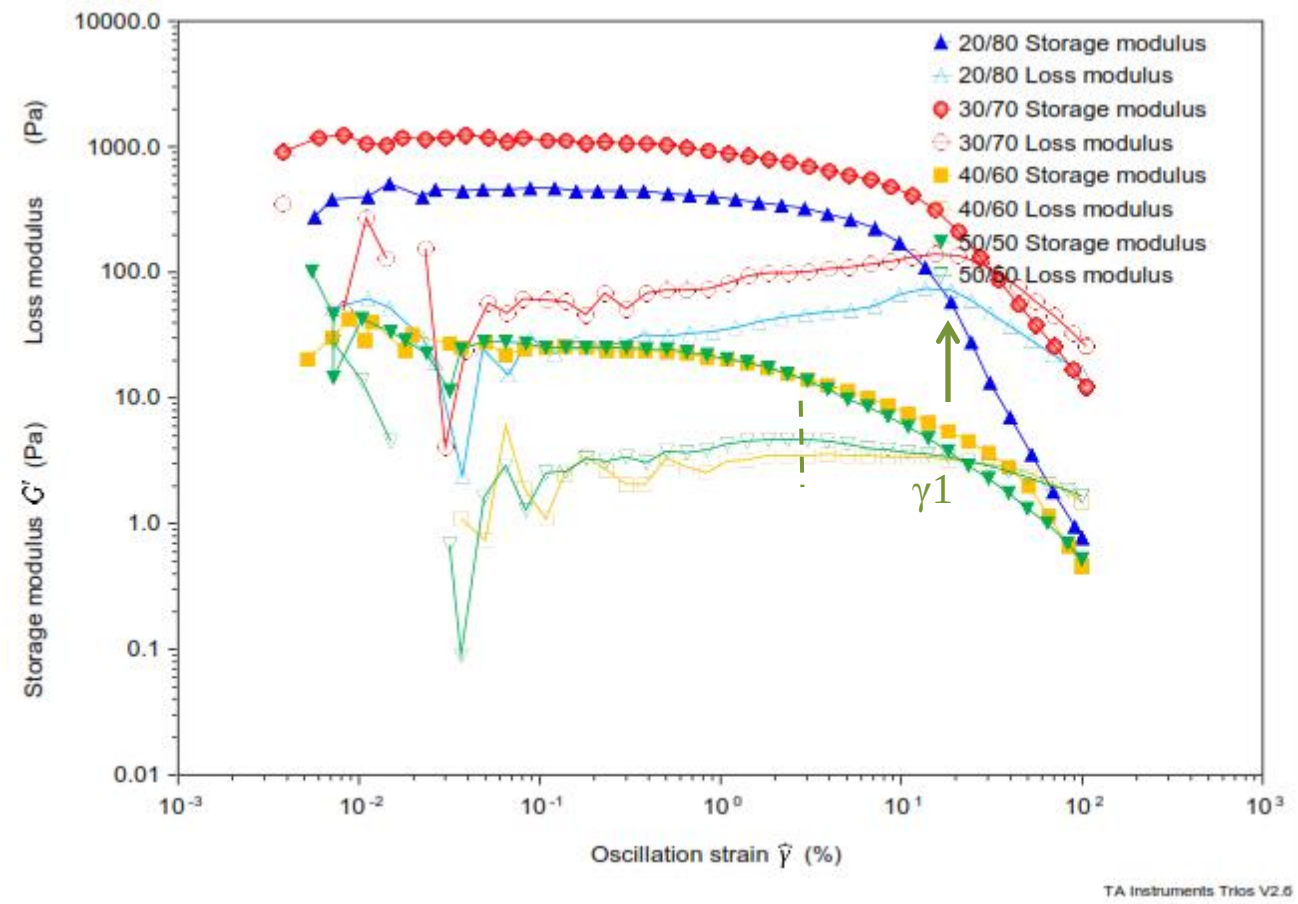

Figure 3.3: Rheology of Pickering emulsion gels with hard shear. Strain sweep profiles for 5% particle volume fraction systems with 20/80, 30/70, 40/60 and 50/50 ratio after hard shear; storage modulus values are denoted by filled symbols; loss modulus values are denoted by open symbols; blue, red, orange and green with respect to 20/80, 30/70, 40/60 and 50/50 ratio.

We also get a set of profiles of strain sweep for each sample after destroying the structure entirely (γ = 10000%). (See Figure 3.3) Different from the original emulsion gels, the system with ratio of 30/70 exhibits larger G', G'' comparing to 20/80 and 40/60. After hard shear the gels and destruct the structure entirely, emulsions exhibit only one peak (dark green arrow) $\gamma 1 \approx 3\%$ for high η; $\gamma 1 \approx 20\%$ for low η. Comparing to the strain sweep profile of original emulsion gels, modulus are overall one magnitude smaller than original group which indicates the degree of destroy from hard shear.

It is consistent with our observation in Chapter 2.

Frequency sweep tests with samples were performed before the oscillatory experimental design. Generally, storage modulus is larger than loss modulus, which shows a tendency of nearly frequency-independence. It is consistent with the behavior of very stable emulsions.

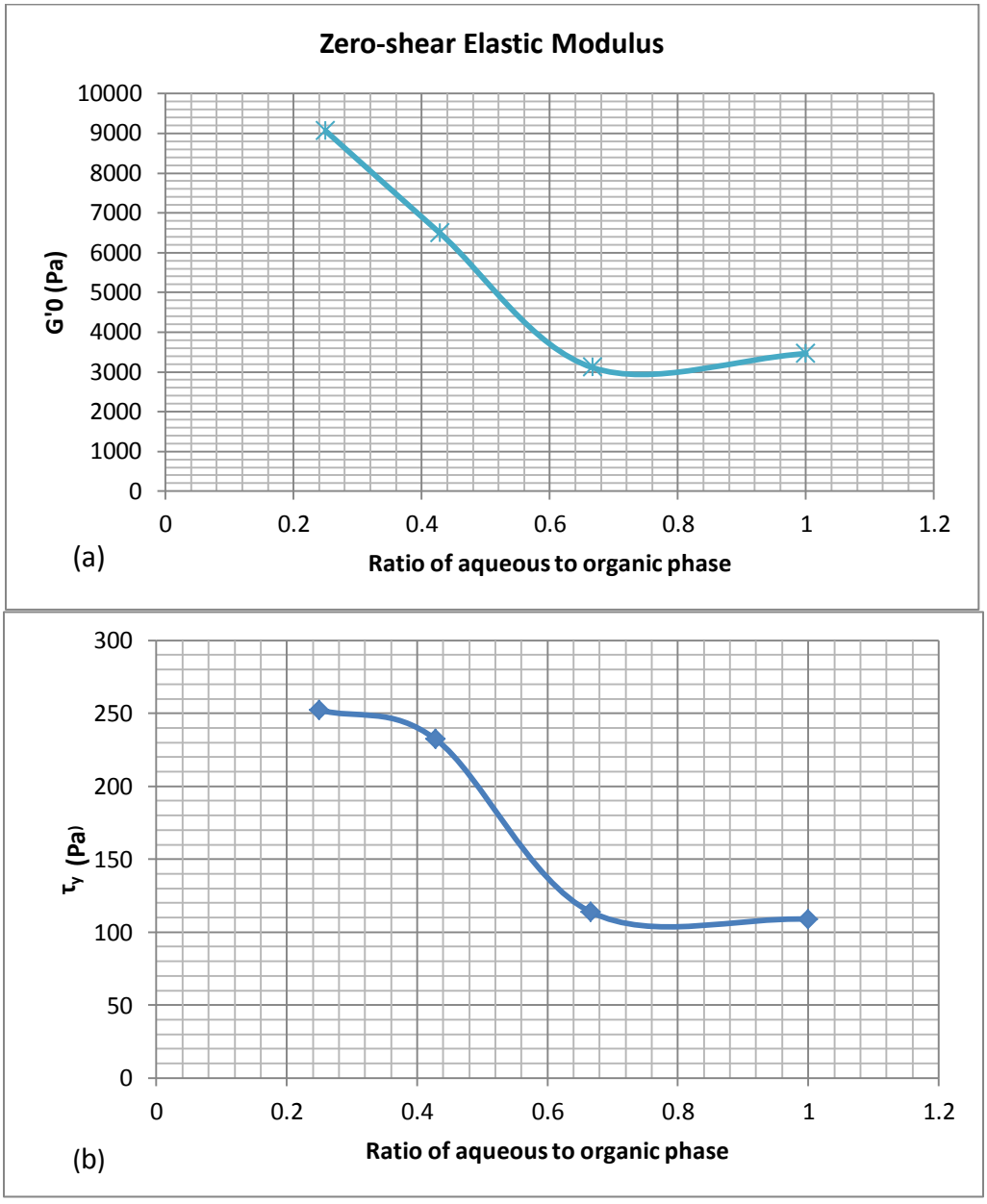

Figure 3.4 a) Zero-shear elastic modulus with ratio of aqueous/organic phases; b) Yield stress with ratio of aqueous/organic phases.

Based on previous rheology tests, the relationships of zero-shear elastic modulus G'_0 and yield stress τ_y with respect to ratio of aqueous to organic phase were investigated. Figure 3.4 exhibited both zero-shear elastic modulus G'_0 and yield stress τ_y having typical signature behavior. The zero-shear elastic modulus in Figure 3.4 (a), G'_0 was estimated as the average value of G' over the range of $0.005\% < \gamma < 0.01\%$. The yield stress in Figure 3.4 (b), τ_y, was defined as the stress value at which G'= G''.

Based on previous study of zero-shear solidlike storage modulus and yield stress, these two parameters both exhibit a relationship as a power-law function of the particle volume fraction[4]. In our work, zero shear modulus G'_0 and yield stress τ_y show a relationship with ratio of aqueous/organic η in colloidal gels. If the ratio of aqueous/organic η is lower than 0.6, these two parameters decrease with increasing ratio; for ratio higher than 0.6, the correlation is uncertain. It indicates that the ratio of aqueous/organic η is a significant determining factor in rheological behavior.

3.2.3 Creeping Test

The coupling effects with respect to instrument inertia and surface elasticity using a controlled stress device could lead to a distinguished damped oscillatory strain response in creeping experiments are known as "creep ringing" [8].

For samples have been at rest for a sufficiently long time, if a constant small stress is applied to, the strain will gradually rise to a limitation. In the final stage, the higher stress is applied, the higher final strain level shown. It is a landmark characteristic of viscoelastic materials, and it could also suggests the gel state[7].

To explore the behavior of our systems (5%, 40/60) with creeping, a test (gap=800 micron) ranging from 0.2Pa to 40 Pa was operated. The results are listed in Figure 3.5 as follows,

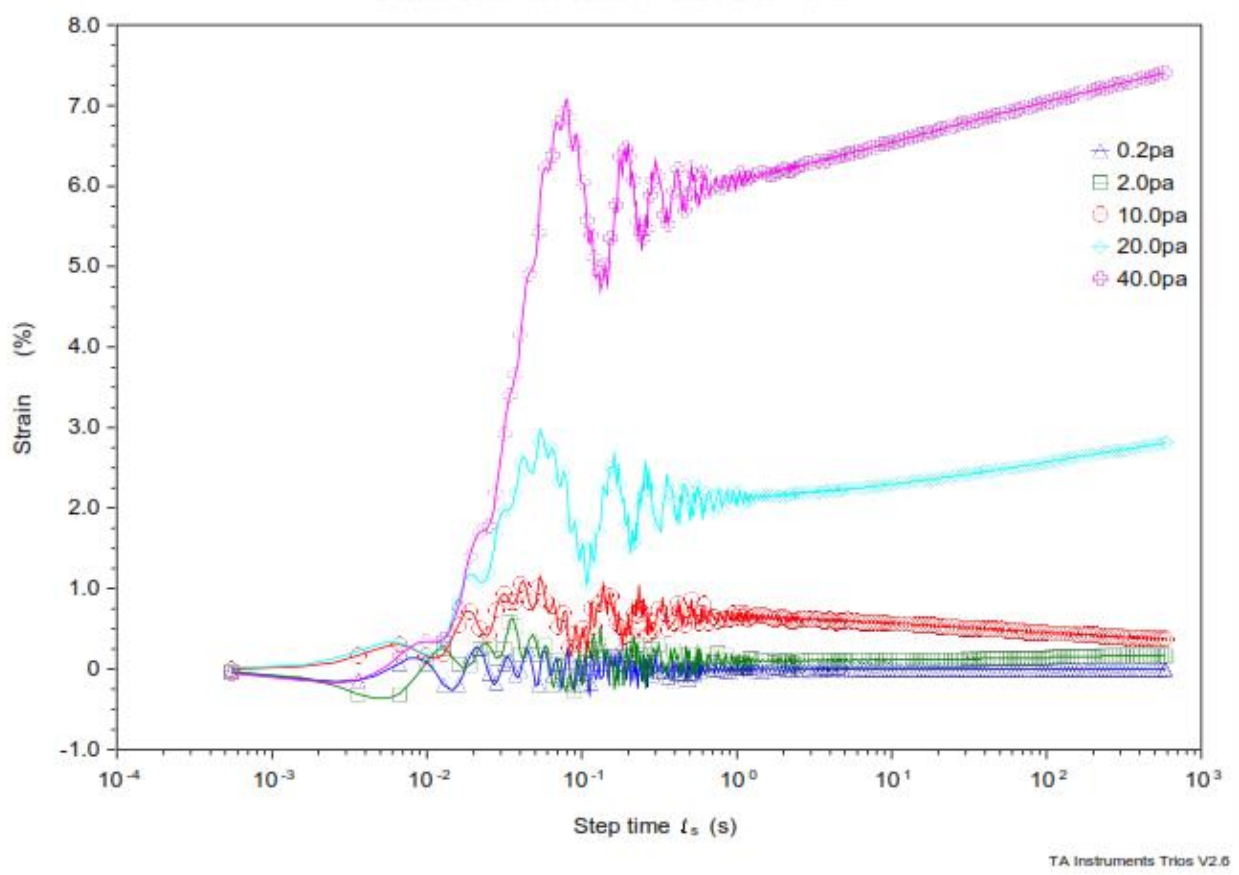

Figure 3.5 Comparison of creeping experiments performed on 5%, 40/60 Pickering emulsion gels with different stresses. Stress range from 0.2 to 40 Pa, spaced logarithmically.

The results from pretest show the viscoelastic nature of the system could cause the strain exhibits a damped vibration phenomenon (creep ringing). The frequency of oscillation could be used to calculate the elasticity of the gels.

Then if we take average droplet size as mentioned in Chapter 2 into consideration, increasing the distance between parallel plates could minimize size effects on creeping. Then we alter the gap to 1000 micron and extend the range of the stress from 1 to 240Pa (Figure 3.6).

We could tell with a large stress (120Pa), our system could still balance to reach the "creep ringing" status. However, when raise stress to 240Pa, creep ringing is ignorable. Tests for the transition between "flow" and "no-flow" could narrow to identify a well defined stress level.

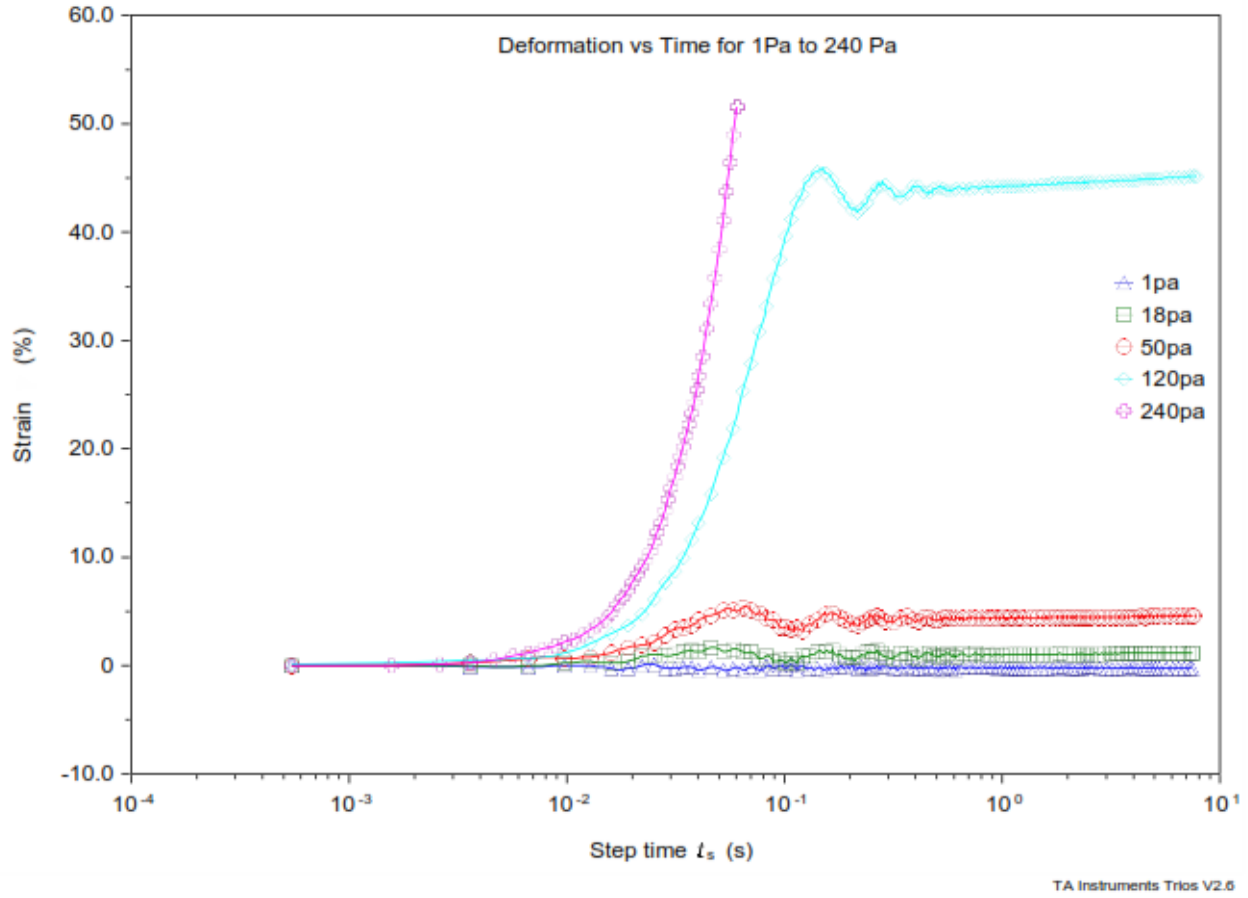

Figure 3.6 Comparison of creeping experiments performed on 5%, 40/60 Pickering emulsion gels with different stresses. Stress ranges from 1 to 240 Pa (1000 micron gap)

3.3 Result Evaluation

In Figure 3.2 and 3.3, storage and loss moduli (G' and G'', respectively) are plotted with an increasing strain. According to Michiel Hermes and Paul S. Clegg[10], there are three different yielding mechanisms in concentrated Pickering emulsions under shear. Based on volume fraction of droplets and interactions between droplets, the three categories are repulsive emulsions with high volume fractions, gel-like attractive emulsions and highly compressed emulsion[10]. As shown in Figure 3.2, the emulsion gel has become stiff enough after ultrasonication (G'>10G''). The two peaks in loss modulus at $\gamma_1 \approx 3\%$, $\gamma_2 \approx 30\%$ could categorize our attracted droplets emulsion gels into the gel-like Pickering emulsions, which also exist in attractive surfactant-stabilized emulsions above random close packing[12]. This similarity between Pickering emulsion gels and surfactant-based emulsion systems indicates that before the attractive emulsions start to fully yield, systems must experience relax first.

When the strain reached 30% for η=20/80, 50% for η=30/70, 60% for η=40/60 and η=50/50, storage and loss moduli crossover at this point. With increasing strain, small droplets merge together and large droplets formed. This structural destroy process lead to decreasing storage and loss moduli (G' and G'').

After hard shear the gels and destruct the structure entirely, emulsions exhibit only one peak $\gamma_1 \approx$ 3% for high η; $\gamma_1 \approx$ 20% for low η. It is similar to the strain-sweep profile of the highly compressed (bi-liquid foam) emulsion system[10]. Comparing to surfactant-stabilized emulsions, the signature peak is close to repulsive emulsions with above random close packing[12]. After hard shear, the observation matches with the mechanism of highly compressed emulsions that droplets coalesce and interface collapse.

M. N. Lee et al. [4] found that zero-shear storage modulus and apparent yield stress both are function of particle volume fraction. Precisely, gels become stronger with higher particle volume fraction and it could be described as a power – law relationship. Particle volume fraction functions as the primary determinant of the rheological behavior[4], despite of different volume ratio of the aqueous to organic phase η. In our emulsion gels, however, volume ratio does influence both zero-shear storage modulus and yield stress in our system, especially for ratio ranging from 0.25 to 0.6 (no data for ratio lower than 0.25).

Creep ringing is caused by the combination of instrument inertia with elasticity of the viscoelastic system. In step-stress and impulse-response experiments, inertial effects are ubiquitous and unavoidable in stress-controlled rheometry[8]. At short time scale, inertia limits the ability to measure the theoretical creep response. If creep ringing can be applied to estimate viscoelastic properties, the accessible range of oscillation tests can be slightly extended[9].

3.4 Summary

Strain-sweep oscillatory measurements were performed within Pickering emulsion gels (η=40/60) with different frequency. Given the storage modulus (G'/Pa) and loss modulus (G''/Pa) of samples, the higher the frequency is, the lower the modulus crossover strain is. Furthermore, strain changes show weak correlation with modulus crossover value. When extend strain-sweep tests to a gradient of ratio (aqueous /organic), the larger the ratio is, the higher the strain of crossover modulus is. After a large shear applied to the structure and ensures it has been destroyed entirely, the second time strain sweep tests were conducted, however, a unique distribution of modulus was shown. This interesting observation indicates that different ratio show different "self-healing" ability in oscillation rheological behavior. Our original emulsion

gels share similar rheological characteristics with gel-like Pickering emulsion[10]; After going through a hard shear, the systems exhibit behaviors like highly compressed emulsions (bi-liquid foam).

Zero shear modulus G'_0 and shear stress τ_y indicate a signature with respect to ratio of aqueous/organic η in colloidal gels. At small stress range, Pickering emulsion gels exhibit "creep ringing" phenomena out of the viscoelastic nature of the system. For large enough stress, the strain increases with increasing stress.

REFERENCE

[1] S. U. Pickering. *J. Chem. Soc. 1907, 91,* 2001.

[2] S. Sacanna, W. K. Kegel, and A.P. Philipse. *Physical Review Letters 2007, 98,* 158301.

[3] F. Leal-Calderon and V. Schmitt. Curr. Opin. Colloid Interface Sci, 2008, 13,217.

[4] M. N. Lee, H. K. Chan, and A. Mohraz. *Langmuir 2012, 28,* 3085.

[5] T. L. Narrow, *Experiments in Fluids* 2000, 28, 282-283

[6] Alexander Ya. Malkin, *Rheology* 2006 52

[7] Jan Mewis, Norman J. Wagner, *Colloidal Suspension Rheology* 2012 201-214, 236

[8] Aditva Jaishankar, Vivek Sharma and Gareth H. McKinley, *Soft Matter* 2011, 7, 7623-7634

[9] Randy H. Ewoldt, Gareth H. McKinley, *The Society of Rheology*, Vol 76, No. 1, Jan 2007

[10] Michiel Hermes and Paul S. Clegg, *Soft Matter*, 2013, 9, 7568

[11] D. Vella, P. Aussillous and L. Mahadevan, Europhysics Letters, 2004, 68(2), 212-218

[12] S.S. Datta, D.D. Gerrard, T.S. Rhodes, T.G Mason and D.A. Weitz, *Phys. Rev. E: Stat, Nonlinear, Soft Matter Phys.*, 2011, 84,041404

[13] Catherine P. Whitby, Lisa Lotte and Chloe Lang, *Soft Matter*, 2012, 8, 7784

[14] Sowmitri Tarimala and Lenore L.Dai, *Langmuir*, 2004, 20, 3492-3494